Genomic Analysis of Circulating Tumor DNA in 3,334 Patients with Advanced Prostate Cancer Identifies Targetable BRCA Alterations and AR Resistance Mechanisms

Hanna Tukachinsky[1], Russell W. Madison[1], Jon H. Chung[1], Ole V. Gjoerup[1], Eric A. Severson[1], Lucas Dennis[1], Bernard J. Fendler[1], Samantha Morley[1], Lei Zhong[1], Ryon P. Graf[1], Jeffrey S. Ross[1,2], Brian M. Alexander[1], Wassim Abida[3], Simon Chowdhury[4], Charles J. Ryan[5], Karim Fizazi[6], Tony Golsorkhi[7], Simon P. Watkins[7], Andrew Simmons[7], Andrea Loehr[7], Jeffrey M. Venstrom[1], and Geoffrey R. Oxnard[1]

ABSTRACT

Purpose: Comprehensive genomic profiling (CGP) is of increasing value for patients with metastatic castration-resistant prostate cancer (mCRPC). mCRPC tends to metastasize to bone, making tissue biopsies challenging to obtain. We hypothesized CGP of cell-free circulating tumor DNA (ctDNA) could offer a minimally invasive alternative to detect targetable genomic alterations (GA) that inform clinical care.

Experimental Design: Using plasma from 3,334 patients with mCRPC (including 1,674 screening samples from TRITON2/3), we evaluated the landscape of GAs detected in ctDNA and assessed concordance with tissue-based CGP.

Results: A total of 3,129 patients (94%) had detectable ctDNA with a median ctDNA fraction of 7.5%; *BRCA1/2* was mutated in 295 (8.8%). In concordance analysis, 72 of 837 patients had *BRCA1/2* mutations detected in tissue, 67 (93%) of which were also identified using ctDNA, including 100% of predicted germline variants. ctDNA harbored some BRCA1/2 alterations not identified by tissue testing, and ctDNA was enriched in therapy resistance alterations, as well as possible clonal hematopoiesis mutations (e.g., in *ATM* and *CHEK2*). Potential androgen receptor resistance alterations were detected in 940 of 2,213 patients (42%), including amplifications, polyclonal and compound mutations, rearrangements, and novel deletions in exon 8.

Conclusions: Genomic analysis of ctDNA from patients with mCRPC recapitulates the genomic landscape detected in tissue biopsies, with a high level of agreement in detection of *BRCA1/2* mutations, but more acquired resistance alterations detected in ctDNA. CGP of ctDNA is a compelling clinical complement to tissue CGP, with reflex to tissue CGP if negative for actionable variants.

See related commentary by Hawkey and Armstrong, p. 2961

Introduction

Prostate cancer is the second most common cancer in men, accounting for 7% of all cancer-related deaths in this population (1). This cancer is driven by androgen receptor (AR) signaling, and androgen deprivation therapy is the first-line treatment for metastatic prostate cancer. Duration of response varies, with a median of 1–2 years before the disease progresses to castration-resistant prostate cancer (2). AR signaling inhibitors (ARSi) for treatment of metastatic castration-resistant prostate cancer (mCRPC) include abiraterone and enzalutamide, but primary and acquired resistance to these agents remain a challenge (3). Taxane-based chemotherapy has demonstrated efficacy prior and postprogression on abiraterone and enzalutamide (4, 5), yet the 3-year overall survival rate for mCRPC remains under 50% (6).

The landscapes of genomic alterations (GA) of primary prostate cancer (7) and mCRPC (8, 9) have been characterized previously using tissue biopsies and are used to identify mechanisms of resistance to ARSis (10–13). Some GAs enriched in mCRPC are emerging as potential therapeutic targets. Genomic profiling of recent specimens that captures somatic alterations may thus be more valuable than sequencing archival, presystemic treatment primary tumor tissue.

The most recent advances in mCRPC therapy target DNA repair defects in mCRPC using PARP inhibitors (PARPi; refs. 14–16). Rucaparib (17) and olaparib have recently been FDA approved for treatment of mCRPC with germline or somatic *BRCA1/2* alterations. Germline alterations in homologous recombination repair (HRR) genes *BRCA1/2* are a hereditary risk factor for prostate cancer (18) and mCRPC samples show enrichment in *BRCA2* alterations compared with primary tumors, suggesting loss of HRR is a therapeutically relevant driver of aggressive disease (19). Loss-of-function alterations in other DNA damage repair (DDR) genes are also enriched in mCRPC and may be targetable with PARPis, but require further investigation (14–16).

While mutational status of DDR genes can be assessed with smaller sequencing panels, wider panels can detect other alterations targetable in mCRPC, such as PI3K pathway perturbations, which have been targeted with ipatasertib (20), as well as genomic signatures, such as tumor mutational burden and microsatellite instability (MSI), that

[1]Foundation Medicine Inc., Cambridge, Massachusetts. [2]Upstate Medical University, Syracuse, New York. [3]Memorial Sloan Kettering Cancer Center, New York, New York. [4]Guy's, King's, and St. Thomas' Hospital, London, England, United Kingdom. [5]University of Minnesota Medical School, Minneapolis, Minnesota. [6]Institut Gustave Roussy, Villejuif, France. [7]Clovis Oncology, Boulder, Colorado.

Note: Supplementary data for this article are available at Clinical Cancer Research Online (http://clincancerres.aacrjournals.org/).

H. Tukachinsky and R.W. Madison contributed equally to this article.

Corresponding Author: Geoffrey R. Oxnard, Clinical Development, Foundation Medicine, Cambridge, MA 02141. Phone: 617-418-2200; E-mail: goxnard@foundationmedicine.com

Clin Cancer Res 2021;27:3094–105

doi: 10.1158/1078-0432.CCR-20-4805

Translational Relevance

Comprehensive genomic profiling (CGP) in metastatic castration-resistant prostate cancer (mCRPC) is of increasing value given the diversity of emerging treatment options. While CGP by tissue testing remains the gold standard, bone metastases are challenging to sample and analyze. Genomic profiling of plasma cell-free circulating tumor DNA (ctDNA) offers a compelling, minimally invasive complement to tissue testing. Advanced prostate cancer has a high shed rate (ctDNA was detectable in 94% of patients). Using the largest cohort of patients with mCRPC to date, we demonstrated high concordance between alterations identified by liquid and tissue biopsy. ctDNA detected additional alterations, including a broad spectrum of androgen receptor resistance alterations and somatic *BRCA1/2* mutations and reversions. ctDNA profiling can overcome the technical difficulties and high failure rates associated with bone metastasis biopsy and help to guide precision therapy in advanced prostate cancer.

predict response to immunotherapy and are FDA-approved biomarkers for pembrolizumab in all solid tumors (21, 22).

Despite the inherent advantages of profiling the latest available sample from a patient with advanced disease, mCRPC presents a technical challenge for collection of a tissue specimen, with metastases often confined to bone (23, 24). Bone biopsies are invasive, technically difficult to collect, and have high failure rates of obtaining enough quality DNA for sequencing (10, 25, 26). Blood-based liquid biopsy and genomic profiling of cell-free circulating tumor DNA (ctDNA) from plasma provide a minimally invasive alternate method to profile mCRPC, with the added capability of detecting variants from multiple metastatic lesions that may have undergone clonal evolution. Here, we build off previous studies of ctDNA in mCRPC (27–31) by analyzing a larger cohort of patients, characterizing the genomic landscape leveraging clinically available approaches, and evaluating concordance with tissue-based CGP.

Materials and Methods

A total of 3,334 liquid biopsy samples and 2,621 tissue samples were assayed with hybrid capture–based comprehensive genomic profiling (CGP). CGP was performed in a Clinical Laboratory Improvement Amendments–certified, College of American Pathologists–accredited, New York State–regulated reference laboratory [Foundation Medicine, Inc. (FMI)]. Patients who submitted screening samples for TRITON2 or TRITON3 provided written informed consent before participation. Approval for the study of the FMI dataset, including a waiver of informed consent and Health Insurance Portability and Accountability Act waiver of authorization, was obtained from the Western Institutional Review Board (protocol 20152817). Studies were conducted in accordance with the Declaration of Helsinki.

Liquid biopsy specimens were obtained from three cohorts: screening samples from the TRITON2 (NCT02952534) and TRITON3 (NCT02975934) trials of rucaparib (collected November 2016–March 2019), and samples submitted to FMI for routine clinical testing (December 2013–March 2019). Cell-free DNA (cfDNA, 20–100 ng) was extracted to create adapted sequencing libraries before hybrid capture and sample-multiplexed sequencing (FoundationACT, FoundationOne Liquid) as described previously (32). Two versions of the plasma assay were used, with 62 (FoundationACT) or 70 genes (FoundationOne Liquid). Genomic regions baited in the two different liquid biopsy assays are depicted in Supplementary Table S1. GAs detected by both assays included base substitutions, insertions and deletions (short variants), rearrangements, and copy-number changes. This study did not evaluate gene deletions. Supplementary Table S2 depicts frequencies of all GAs assessed by liquid biopsy in the three different datasets.

Tissue specimens from metastatic sites submitted for routine clinical testing (December 2013–March 2019) were used for global comparisons of liquid biopsy with metastatic tissue ($N = 2{,}006$). Additional tissue specimens used only in the concordance analysis were screening samples collected from the TRITON2 ($N = 337$) and TRITON3 ($N = 277$). At least 50 ng of DNA was isolated from prostate cancer acinar adenocarcinoma formalin-fixed, paraffin-embedded tumor specimens and sequenced to high, uniform ≥500× coverage, with larger gene panels inclusive of all 70 genes in liquid assays.

MSI status was determined in samples screened with the 70-gene panel, as described previously (33). For tumor specimens, zygosity and somatic/germline status for mutations were computationally predicted without matched normal tissue, as described previously (34); in validation testing of 480 tumor-only predictions against matched normal specimens, accuracy was 95% for somatic and 99% for germline predictions (35).

Quantification of the ctDNA fraction was measured using two complementary methods: the proprietary tumor fraction estimator (TFE) and the maximum somatic allele frequency (MSAF) method. TFE is based on a measure of tumor aneuploidy that incorporates observed deviations in coverage across the genome for a given sample. Calculated values for this metric are calibrated against a training set based on samples with well-defined tumor fractions to generate an estimate of the tumor fraction. When lack of tumor aneuploidy limits the TFE's ability to return an informative estimate, MSAF is used. MSAF calculates the allele fraction of all known somatic, likely somatic, and variant of unknown significance substitution alterations detected at >2,000× median unique coverage by non-PCR duplicate read pairs, excluding germline variants and variants associated with clonal hematopoiesis.

Results

Patient characteristics and ctDNA shed

Liquid biopsy CGP results from a total of 3,334 patients with prostate cancer were included. Patients screened for TRITON3 ($n = 818$) had progressed on one prior ARSi therapy, while patients screened for TRITON2 ($n = 856$) progressed on—one to two lines of ARSis, followed by a taxane-based chemotherapy in the castration-resistant setting. A total of 1,660 liquid biopsies were sourced from routine clinical testing at FMI of patients with advanced prostate cancer. The median age of patients was 72 years [range, 38–97; interquartile range (IQR), 66–78] and was similar across all three datasets (**Table 1**; Supplementary Fig. S1).

Screening samples from the clinical trials contained detectable ctDNA in >95% of samples (as determined by the comprehensive tumor fraction estimation method, see Supplementary Data for full method description). The median ctDNA fraction of these datasets was 7.5% (IQR, 0.8%–34%; **Table 1**; **Fig. 1A**) and was higher in patients who had progressed on taxane (median, 18.1% in TRITON2 vs. 3.4% in TRITON3), consistent with higher ctDNA shed after more lines of therapy (29). The number of samples with no ctDNA detected (i.e., no detection of aneuploidy or somatic alleles of known or unknown functional significance) was 40 of 746 (5.4%) in the TRITON3

Table 1. Patient characteristics in the three liquid biopsy datasets.

Liquid biopsy datasets and metastatic tissue biopsy dataset used as comparison (unmatched)										
		Liquid biopsies								Tissue biopsies
		FMI routine clinical cohort		TRITON2 screening cohort		TRITON3 screening cohort		Total		Metastatic tissue biopsies
Cohort characteristics		Prostate cancer plasma samples submitted for CGP during routine clinical care		mCRPC, progressed on 1–2 next-generation ARSi and taxane-based chemotherapy		mCRPC, progressed on 1 next-generation ARSi		—		Prostate cancer tissue samples submitted for CGP during routine clinical care
Patients, *N*		1,660		856		818		3,334		2,006
Profiled with FACT, *n*	Profiled with F1L, *n*	943	717	106	750	72	746	1,121	2,213	—
Median patient age, years (range)[a]		71 (38–≥89[b])		72 (46–95)		73 (43–97)		72 (38–97)		69 (39–≥89[a])
Median ctDNA fraction, % (IQR)		7.7 (0.6–35.7)		18.1 (1.5–38.1)		3.4 (0.8–23.3)		7.5 (0.8–33.7)		—
Percentage of samples with no ctDNA detected in sample		8.6% (142/1,660)		2.7% (23/856)		4.9% (40/818)		6.1% (205/3,334)		—
Percentage of samples with ctDNA fraction of ≥20%		39% (648/1,660)		47% (401/856)		28% (233/818)		38% (1,282/3,334)		—
1 or more oncogenic/deleterious GAs detected in sample[c]		85.6% (614/717)		90.3% (677/750)		80.0% (597/746)		85.3% (1,888/2,213)		99.2%[d] (1,991/2,006) 89.6%[e] (1,797/2,006)
MSI-H detected[c]		1.12% (8/717)		2.00% (15/750)		1.07% (8/746)		1.40% (31/2,213)		2.74% (55/2,006)
Site of metastatic biopsy		N/A		N/A		N/A		N/A		
Bone										36.7%
Liver										34.3%
Other visceral sites										29.0%
Subset of patients with available matched tissue										
Patients with matched tissue, *N*		223		337		277		837		
Profiled with FACT, *n*	Profiled with F1L, *n*	155	68	52	285	27	250	234	603	
Patients with matched tissue collected within 30 days of liquid biopsy, *N*		36		53		28		117		
Profiled with FACT, *n*	Profiled with F1L, *n*	26	10	10	43	2	26	38	79	
Median Δ between liquid and tissue collection, months (IQR)		11 (0.1–44)		31 (5–74)		30 (12–70)		25 (3–61)		

Abbreviations: FACT, FoundationACT; F1L, FoundationOne Liquid.

[a]A total of 28 samples had no available age information: one from routine clinical cohort, 15 TRITON2, and 12 TRITON3 screening samples.

[b]FMI routine clinical datasets do not include specific patient age above 89.

[c]Only samples analyzed with F1L (70-gene panel) used for this comparison.

[d]Oncogenic/deleterious GAs in all genes baited in tissue biopsy panel considered.

[e]Oncogenic/deleterious GAs only in genes baited in 70-gene liquid panel considered.

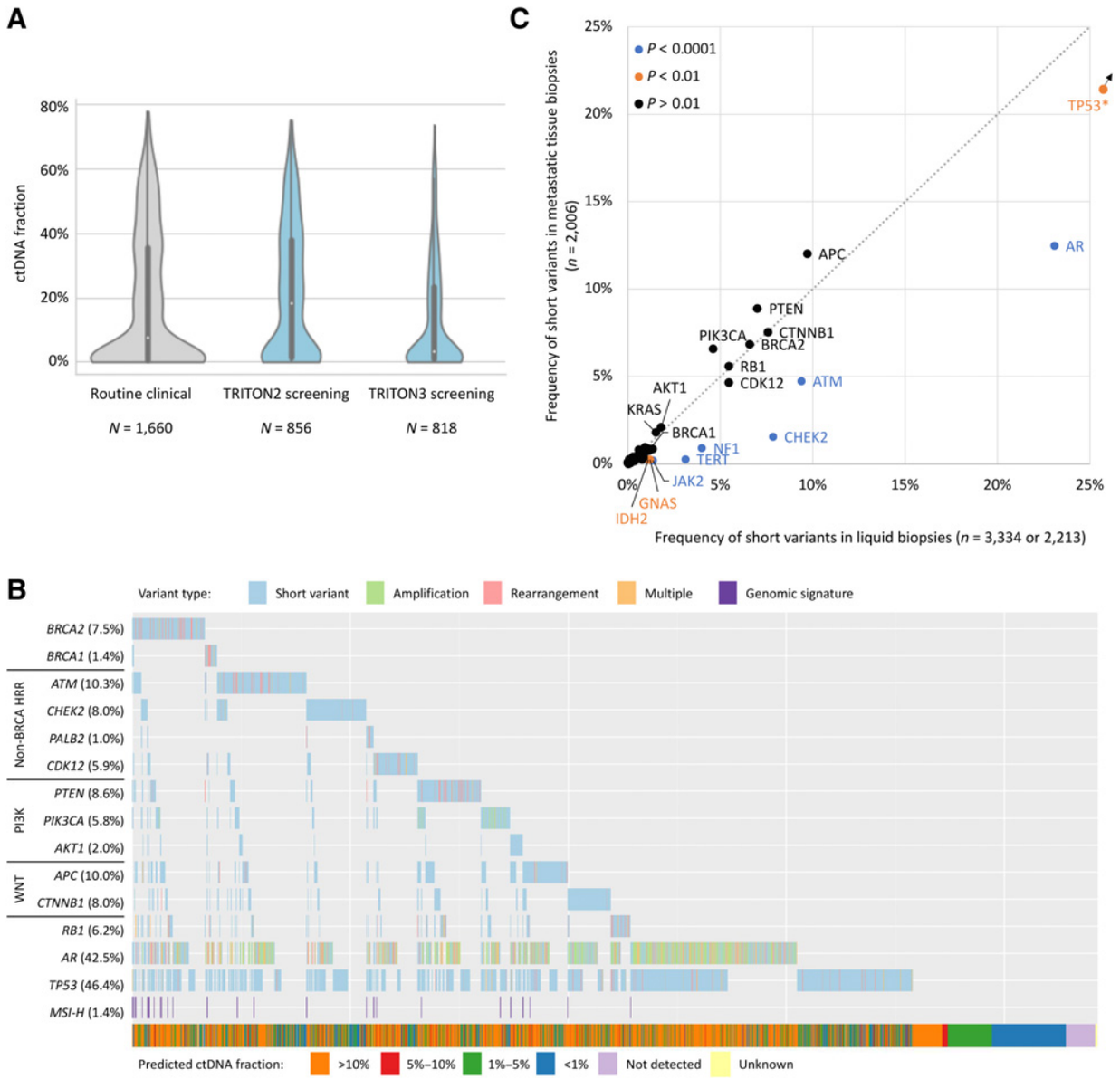

Figure 1.

Genomic landscape of prostate cancer in liquid biopsies. **A,** Distribution of estimated tumor fraction within each liquid biopsy dataset. **B,** Frequency and cooccurrence of alterations in genes associated with mCRPC across 2,213 liquid biopsy samples assayed with 70-gene panel. Variant type is indicated by color legend at the top of the oncoprint. MSI-H status is indicated in last row. Estimated tumor fraction is indicated by bar below the oncoprint. Copy-number deletions were not reported by the liquid biopsy assay versions used in this study. **C,** Frequency of short variants detected in metastatic tissue samples versus frequency of short variants detected in liquid samples. Genes with short variants with significantly different frequencies in tissue and liquid are color coded to reflect *P* value. **TP53* off-scale (45.4% in liquid vs. 40.8% in tissue; $P = 0.0096$). MSI-H, microsatellite instability high.

screening cohort and only 23 of 856 (2.7%) in the more heavily treated TRITON2 screening cohort. A substantial 401 of 856 (47%) samples of the TRITON2 screening cohort had a ctDNA fraction of 20% or above, which allowed for >90% sensitivity of detection for all three variant types reported by the liquid biopsy assay: substitutions/indels, rearrangements, and amplifications. Liquid biopsy identified at least one GA predicted to have deleterious/oncogenic effects on protein function in 2,651 of 3,334 (79.5%) of all patients and 1,888 of 2,213 (85.3%) of patients profiled using the 70-gene panel (**Table 1**).

Genomic landscape of prostate cancer ctDNA

The most frequently altered genes were *TP53* (46%) and *AR* (42%; **Fig. 1B**; Supplementary Fig. S2A), consistent with patient cohorts with prior ARSi exposure; both genes are commonly altered in tissue-based profiling of mCRPC and associated with resistance to ARSis (36, 37). At least one DNA repair gene was altered in 30% of all patients, including *BRCA2* (7.5%) and *BRCA1* (1.4%). Genes in the PI3K/AKT/mTOR pathway were altered in 14% of samples, including activating mutations in *PIK3CA* and *AKT1* (Supplementary Fig. S3A).

WNT/β-catenin pathway genes were altered in 17% of patients (Supplementary Fig. S3B). Alterations in RAS/RAF/MEK pathway components were detected in 5% of all patients (Supplementary Figs. S2A and S3C). Amplifications of *FGFR1* were detected in 3% of patients, and 11 patients harbored rearrangements of *FGFR1/2/3* with breakpoints in intron 17, which preserve the kinase domain and are predicted to be oncogenic (ref. 38; Supplementary Fig. S3D). MSI-H status was found in 31 of 2,213 (1.4%) of patients (**Table 1**), comparable with the 2% of primary site and 3% of metastatic tissue biopsies (10, 12).

The landscape of short variants (substitutions and indels) detected by liquid biopsy closely resembled the landscape detected in tissue biopsies from metastatic sites of origin (**Fig. 1C**; Supplementary Fig. S4A) and previous reports (9, 11, 12). Rearrangements in most genes were detected at similar frequencies in liquid biopsies relative to metastatic tissue (Supplementary Fig. S4B), except *AR*, as discussed further on. Copy-number amplifications were detected less frequently in liquid than tissue biopsy (Supplementary Fig. S4C), likely owing to decreased sensitivity of detection in samples with low levels of ctDNA (Supplementary Fig. S5). We examined the subset of samples with ≥20% ctDNA fraction (a threshold where there is >95% sensitivity of detection for amplifications; ref. 32). This subset included 1,282 of 3,334 (38%) of all samples (**Table 1**). Amplifications were detected with significantly higher frequency in this subset: *AR* (344/781; 41%), *FGFR1* (91/1,282; 7.1%), and *MYC* (67/1,282; 5.2%). It is important to note that the two liquid biopsy platforms used in this study did not report copy-number losses, and common driver *TMPRSS2-ERG* fusion was not reported because of lack of baiting in these genes.

Frequencies of short variants in liquid biopsies were compared with those in 2,006 metastatic tissue biopsies (**Fig. 1C**). While most genes were altered at similar rates, variants were detected significantly more often in liquid in 9 of 70 genes. Alterations in *AR* were enriched in ctDNA, likely representing resistance mechanisms acquired on therapy. Low level enrichment for *JAK2, GNAS*, and *IDH2* (genes not often altered in mCRPC) likely represents signal from clonal hematopoiesis (39), rather than the tumor; the same applies to mutations in *NF1* and the *TERT* promoter. Alterations in *CHEK2, ATM*, and *TP53* occurred with some frequency in mCRPC tissue biopsies, but were also more prevalent among liquid biopsies; it is uncertain whether this is related to mCRPC biology or also to clonal hematopoiesis, as these have been detected in some studies of clonal hematopoiesis (31). In this study, no strong associations with age were observed for likely clonal hematopoiesis variants in *JAK2, GNAS*, and *IDH2* (Supplementary Fig. S6), thus age association could not be used to distinguish clonal hematopoiesis variants from liquid-prevalent resistance mutations, such as *AR*, sourced from the tumor. The lack of age association for clonal hematopoiesis variants may be the result of an older cohort, in which 88% of patients were older than 60 years.

Overall concordance between tissue and liquid biopsies

Patient-matched tissue samples were available for 837 of the 3,334 liquid biopsies (**Table 1**). Tissue specimens were collected a median of 758 days before plasma collection (range, 19.9 years before to 1.8 years after liquid biopsy; **Table 1**; Supplementary Fig. S7A). A total of 117 pairs were collected within 30 days of each other and were considered "contemporaneous pairs" in this concordance analysis.

Detection of short variants in genes included in the liquid assay showed 75.3% positive percentage agreement (PPA) to tissue as reference (Supplementary Table S3). PPA was 70.3% for rearrangements and 27.5% for amplifications. Among contemporaneous pairs, PPA increased to 87.2%, 91.7%, and 38.8% for short variants, rearrangements, and amplifications, respectively. ctDNA fraction was a major factor in concordance of liquid to tissue for amplifications because 20% ctDNA fraction is needed to detect amplifications with >95% sensitivity (32); above this threshold, PPA for amplifications was 50.8%. Alterations exclusively detected in tissue tended to be in sample pairs with a low ctDNA fraction in the liquid biopsy (Supplementary Fig. S7B).

BRCA1/2 alterations

BRCA1/2 was altered in 8.9% of all patients' plasma samples (7.5% *BRCA2*, 1.6% *BRCA1*, and 0.18% both genes). Curiously, *BRCA2* was altered significantly more frequently in the TRITON2 versus TRITON3 screening cohorts (Supplementary Table S4). *BRCA2* inactivation is a predictor of poor response to docetaxel (40, 41), and patients screened for TRITON2 had progressed on a taxane-based chemotherapy, which could account for a larger proportion of these patients in this cohort. *BRCA1* alterations were also more frequent in the group that had received prior taxane. The combined *BRCA1/2* alteration frequency within the TRITON2 screening cohort was 12.3%, nearly twice the frequency in the TRITON3 screening cohort (6.4%; **Fig. 2A**).

Frameshifts were the most common alteration in both *BRCA2* and *BRCA1*, rearrangements were more common in *BRCA1*, and the frequencies of nonsense and missense mutations were similar between the two genes (**Fig. 2B**). A total of 90% of *BRCA1/2*-altered patients had a single mutation detected (**Fig. 2C**). In 10 of the 30 patients with two or more mutations, the additional variants were reversions. All 10 patients with *BRCA1/2* reversions were from the routine clinical CGP dataset, not the TRITON2/3 screening cohorts (**Fig. 2A**), and may have had exposure to platinum-based chemotherapy or PARPis (42–44). Reversions were defined as in-frame deletions spanning a frameshift or nonsense mutation, or missense mutations in the same position as the nonsense mutation (Supplementary Table S5). These alterations were mostly subclonal in relation to the deleterious mutation, with up to 13 found in one sample (**Fig. 2D**).

Studying the variant allele fractions (VAF) of *BRCA1* and *BRCA2* short variants as compared with ctDNA fraction (**Fig. 2E**), two distributions were seen, consistent with somatic and germline mutations. Variants with a VAF ≥ 40% detected at low ctDNA fraction were enriched for putative germline variants (i.e., founder mutations). When ctDNA fraction was high, somatic and germline variants were not clearly distinguishable. Some somatic variants tracked closely with ctDNA fractions, while others appeared subclonal (variants close to the horizontal axis in **Fig. 2D**). The VAF distribution of variants in additional DDR genes, *ATM, CHEK2, PALB2*, and *CDK12*, is provided in Supplementary Fig. S8.

BRCA1/2 variant detection by liquid and tissue biopsy

Among 837 patients in the concordance analysis, 92 (11%) had a *BRCA1/2* alteration detected by one or both assays. A total of 67 (8%) patients had *BRCA1/2* alterations detected concordantly in tissue and liquid, five (0.6%) exclusively in tissue biopsy, and 20 (2.4%) exclusively in the liquid biopsy (**Fig. 3A** and **B**). The PPA between the tissue and liquid assays was 93.1% on the patient level (**Fig. 3B**). The variant-level concordance between the tissue and liquid assays for *BRCA1/2* was high: the PPA was 95.2% and 85% in the TRITON2 and TRITON3 screening cohorts, respectively (Supplementary Table S3).

Lack of detection of *BRCA1/2* variants in liquid was mostly attributable to low ctDNA fraction: of 5 patients with tissue-only detection of a *BRCA1/2* alteration, 4 patients had ctDNA fractions of ≤1% (**Fig. 3A**). Some *BRCA1/2* alterations identified exclusively in the liquid biopsy (colored red in **Fig. 3A**) potentially represent alterations

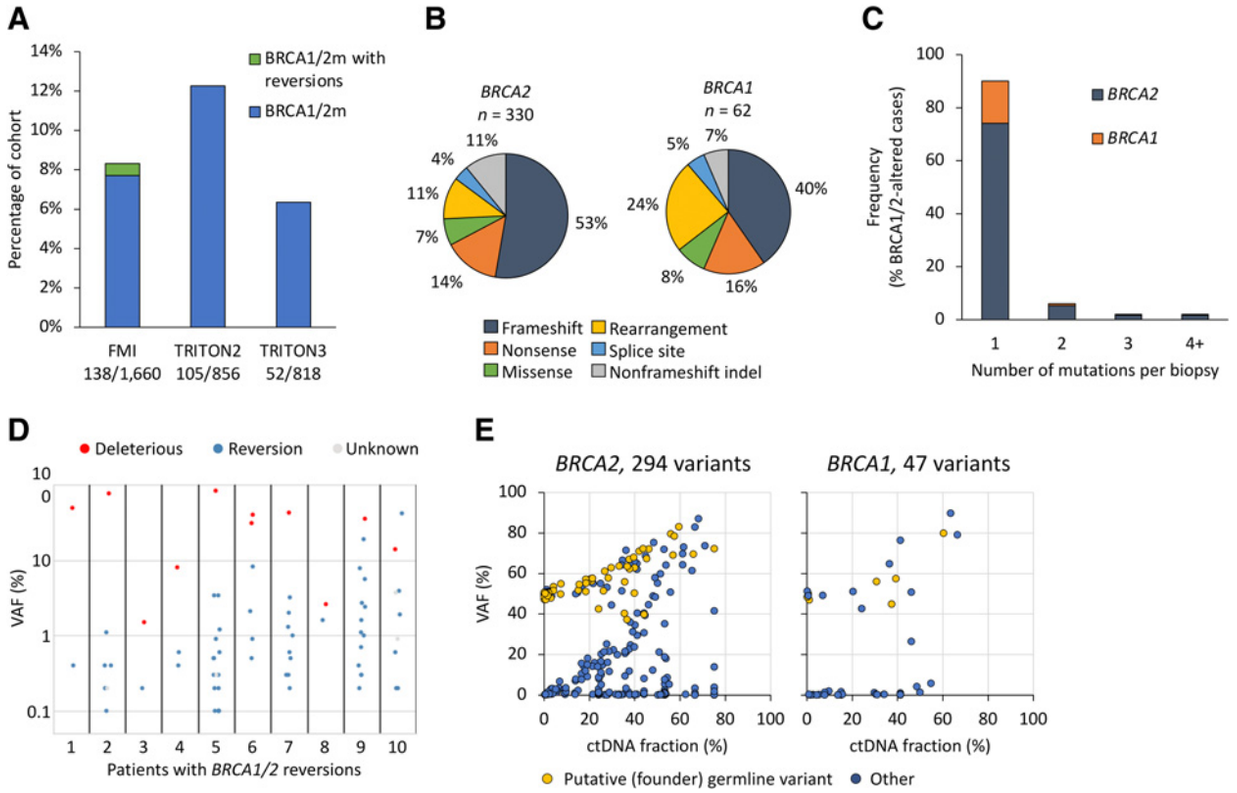

Figure 2.

BRCA1/2 alterations in liquid biopsy. **A,** Prevalence of *BRCA1/2* alterations in the three cohorts. **B,** Types of detected *BRCA1/2* alterations. A total of 174 frameshifts among 157 patients for *BRCA2*, 25 frameshifts among 25 patients for *BRCA1*, 58 *BRCA1/2* nonsense point mutations among 57 cases, 51 patients with rearrangements, 28 missense mutations among 22 patients, 16 splice site alterations among 14 patients, and 49 nonframeshift deletions among 7 patients (these indels were all reversion mutations). **C,** Numbers of *BRCA1/2* alterations per patient. **D,** Variant allele frequencies of *BRCA1/2* short variants in 10 patients with detected reversion mutations. Variants with unknown functional status are splice site mutations. See Supplementary Table S2 for details. **E,** Variant allele frequencies of short variants in *BRCA1* and *BRCA2* compared with the ctDNA fraction of the liquid biopsy. Germline variants were predicted using heuristic scoring of observed instances across all FMI datasets.

acquired after tissue specimens collection (median time difference in sample collection was 38 months; IQR, 15–112; Supplementary Fig. S7C). These variants, especially in *BRCA1*, were more likely to be subclonal, have VAFs significantly smaller than the ctDNA fraction of the sample. However, in five of the 20 samples where only liquid biopsy identified *BRCA1/2* alterations, *BRCA2* short variant VAF exceeded 50% of the ctDNA fraction.

BRCA1/2 alterations detected in tissue were predicted to be germline or somatic, using a previously established and validated computational method (34). All 40 predicted germline mutations were detected in the corresponding liquid biopsies at >40% VAF (**Fig. 3C** and **D**). Sixteen of 18 predicted somatic and eight of 10 unknown status were detected in the corresponding liquid biopsy (**Fig. 3C**), usually at lower VAF (**Fig. 3D**).

Overall, liquid biopsy was able to detect 100% of predicted germline *BRCA1/2* alterations and reliably detect somatic alterations identified in tissue when ctDNA fraction was more than 1%. In samples where *BRCA1/2* VAF was lower than ctDNA fraction, it is possible that the variant represents a subclone, a monoallelic alteration, or even clonal hematopoiesis. It is worth noting the assays used in this study detected inactivating short variants and rearrangements, but did not report *BRCA1/2* copy loss, thus copy-number deletions were not considered in concordance analysis.

Putative and novel resistance AR alterations

Liquid biopsy detected 1,090 *AR* alterations among 42% of evaluated patients (940/2,213). Among *AR*-altered patients, 45% had missense mutations, 33% had amplifications, 8% had rearrangements, and 14% had multiple types of alterations (**Fig. 4A**). *AR* amplifications were identified in 419 patients (43% of *AR*-altered patients and 13% overall), with technically limited detection in samples with low ctDNA fractions (Supplementary Fig. S9). Among the subset of patients with ≥20% ctDNA fraction in their biopsy, *AR* amplifications were detected in 41% (344/781).

Among patients with a mutation or rearrangement in *AR*, approximately 40% harbored ≥2 variants (up to six; **Fig. 4B**; Supplementary Fig. S2B). Many mutations were subclonal, with VAFs smaller than ctDNA fractions; some VAFs exceeded ctDNA fraction, which may result from mutations in amplified copies of *AR* (Supplementary Fig. S10). Hotspots concentrated in the ligand binding domain (LBD) and are known to confer resistance to ARSis (**Fig. 4C**; ref. 45). The most frequent mutations included W742L/C (bicalutamide resistance), H875Y, F877L and T878A (bicalutamide/enzalutamide/apalutamide resistance and promiscuous activation by progesterone), and L702H (resistance to abiraterone/enzalutamide, as well as the AR proteolysis-targeting chimera ARV-110, and activation by corticosteroids; refs. 45, 46). Less common *AR* resistance

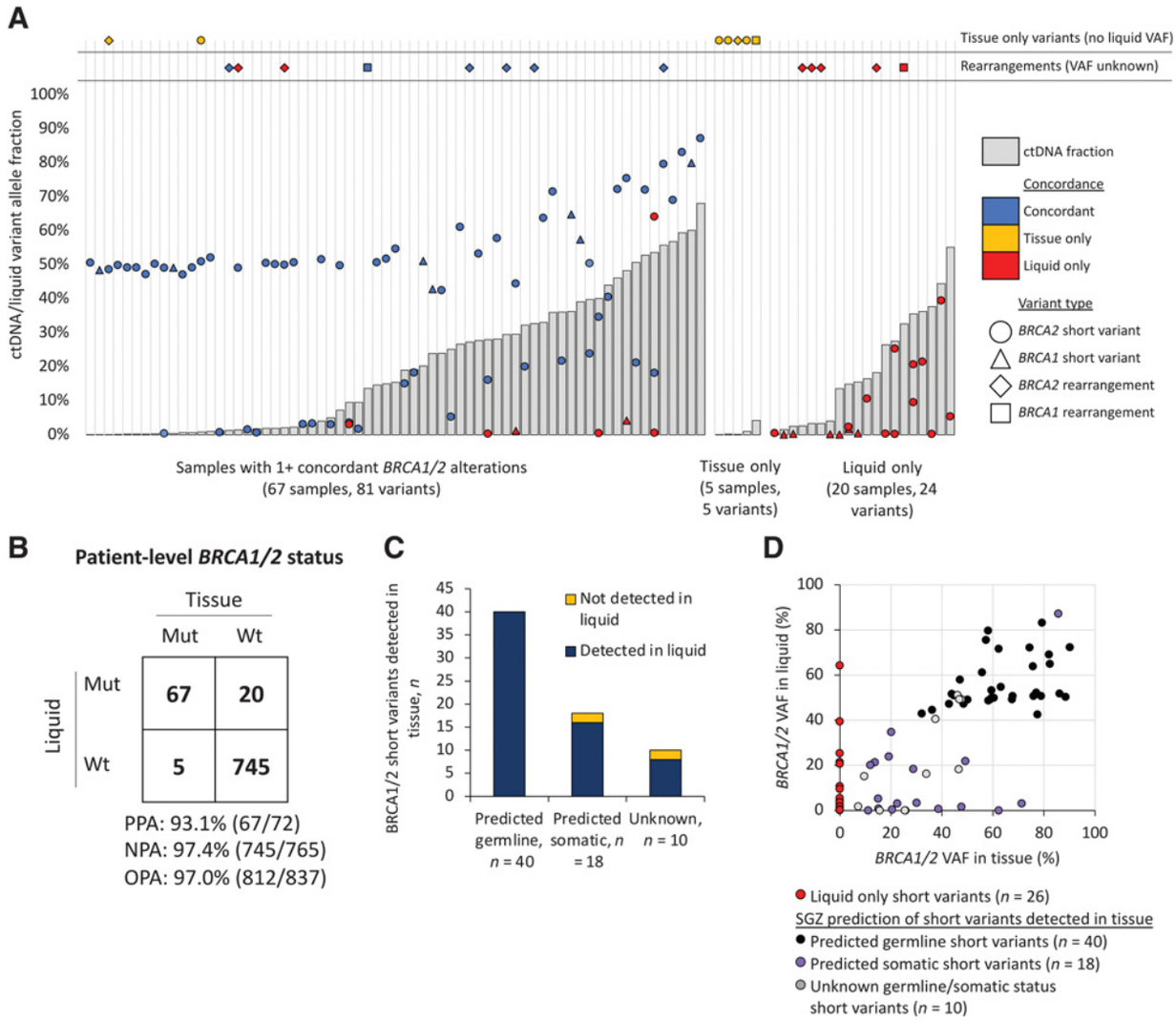

Figure 3.

Concordance of BRCA1/2 detection in liquid and tissue biopsy. **A,** A total of 92 tissue/liquid pairs were available where *BRCA1/2* variants were detected among the tissue sample alone ($n = 5$), the liquid sample alone ($n = 20$), or both ($n = 67$). Samples in each group are arranged in ascending ctDNA fraction (gray bar). Variant allele frequency is indicated for each short variant. Rearrangements, for which VAF was not reported, are indicated at the top of the chart. Tissue-only variants, with no associated liquid VAF, are also indicated at the top of the chart. For simplicity and clarity, all analyses presented in this figure omit nine *BRCA* reversion mutations detected in one sample. All alterations presented are predicted deleterious to *BRCA1/2* function. **B,** Patient-level *BRCA1/2*-mutant status was assigned in the presence of at least one deleterious alteration in *BRCA1* or *BRCA2* in a sample. No patient in this study had multiple discordant *BRCA1/2* variants assigned in tissue and liquid tests. PPA: the number of patients assigned *BRCA1/2*-mutant status by both liquid and tissue biopsies divided by the total number of *BRCA1/2*-mutant patients identified by tissue biopsy. Negative percentage agreement (NPA) was also calculated, with tissue biopsy taken as standard. OPA was calculated as patients assigned similarly by both tests divided by total patients in paired comparison. **C,** SGZ algorithm predictions of variants germline/somatic status using the tissue biopsy, and the proportions of these variants also detected in the matching liquid biopsy. **D,** Comparison of VAF of short variants in liquid versus matched tissue biopsy. Variants were classified as detected in liquid only or detected in tissue. mut, mutant; OPA, overall percent agreement; SGZ, somatic-germline-zygosity; wt, wild-type.

mutations were found in V716M (15 patients), S889G (15 patients), and M896I/V/L (10 patients; **Fig. 4C**); these mutations have been detected in ctDNA from patients with mCRPC who progressed on bicalutamide or abiraterone (45, 47, 48).

Rare *AR* variants were detected in this large dataset, some of which have not been described previously and warrant further characterization. Double mutant F877L/T878A appeared in 11 patients (**Fig. 4D**). This compound mutant has been shown to confer synergistic resistance to enzalutamide in preclinical studies (45, 49). In-frame deletions spanning residues H875 to T878 were detected in 11 patients, each shifting S885 into the T878 position (**Fig. 4D**). While it is not known whether these mutants mimic T878S, their appearance in multiple patients in this study raises the possibility of their being a mechanism of ARSi resistance. One patient harbored indel S647–648>F, impacting critical serine residues within a binding motif for the ubiquitin ligase SPOP, and predicted to stabilize the AR by reducing proteasomal degradation (ref. 50; Supplementary Fig. S11A).

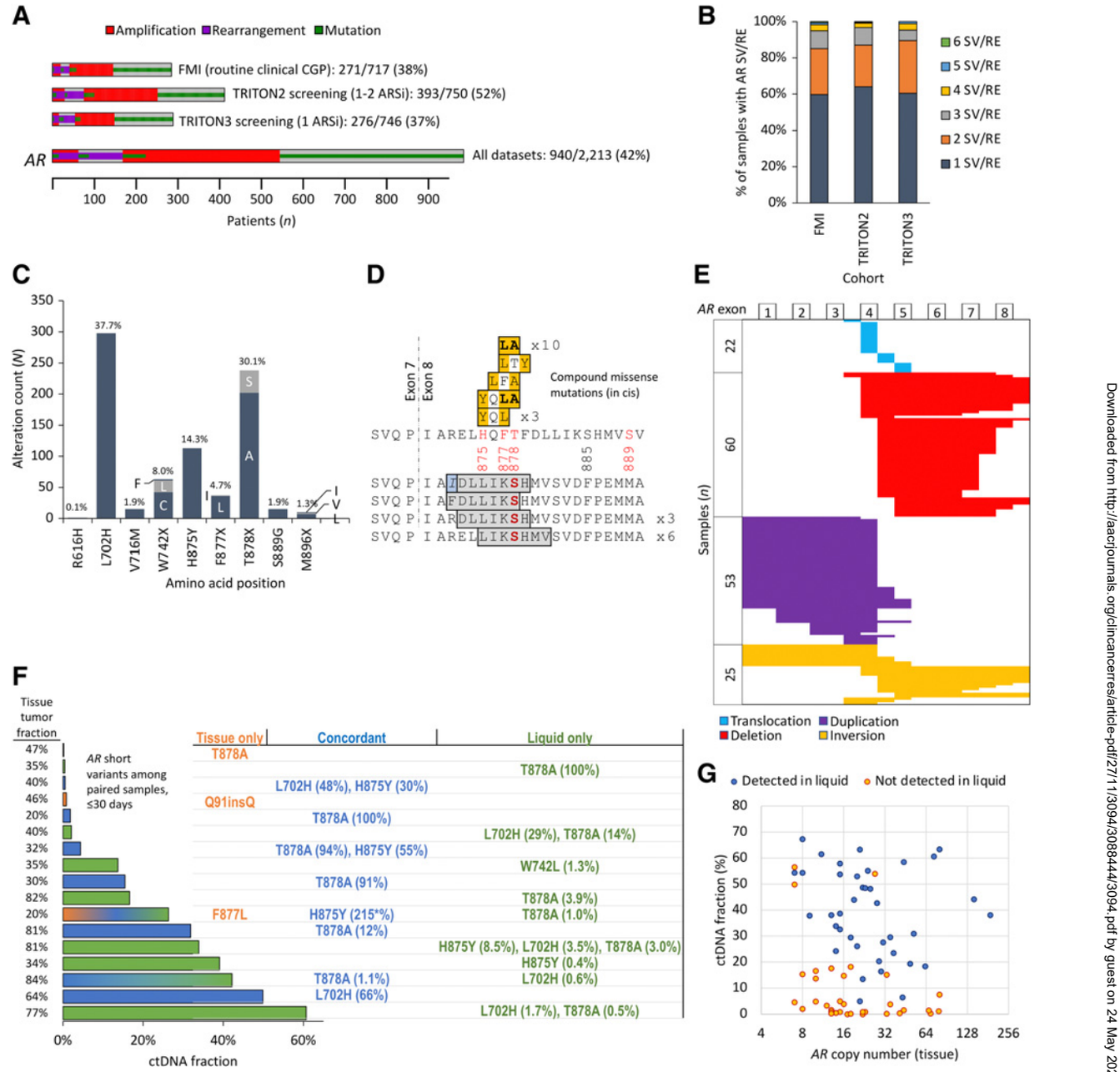

Figure 4.

AR alterations in liquid biopsy. **A,** Oncoprints of 940 *AR*-altered samples, divided as separate cohorts and the aggregate. **B,** Polyclonality of AR-activating mutations: numbers of *AR* short variants and rearrangements per sample. SV, short variant; RE, rearrangement. **C,** Distribution of oncogenic missense mutations in *AR*. Letters indicate amino acid change when there is >1 missense mutation at the position. **D,** Rare *AR* alterations identified near the C-terminus of the LBD: compound missense mutations in cis (gold) and in-frame deletions (gray) spanning important androgen-binding residues H875, F877, and T878, all resulting in S885 moving into the 878 position (red). One sample contained an isoleucine insertion (light blue). F877L/T878A double mutants are predicted to have enhanced resistance to enzalutamide (bold). Sixteen compound mutations were found in 12 patients, and 11 in-frame deletions among as many patients. All patients were confirmed to have progressed on at least one of abiraterone, enzalutamide or apalutamide, except 2 patients with compound mutations for whom treatment information was not available. **E,** Map of *AR* rearrangements that describes breakpoints for translocations and deleted, duplicated, or inverted regions (22 translocations, 60 deletions, 53 duplications, and 25 inversions). *X*-axis is a schematic representation of the eight exons in the *AR* gene (not to scale). Among the 160 patients with *AR* rearrangements, 138 were confirmed to have progressed on at least one of abiraterone, enzalutamide, or apalutamide, and 22 had no available treatment information. **F,** Patient-matched sample pairs collected within 30 days of each other with ≥1 *AR* short variant detected, in ascending order of ctDNA fraction. Bar represents estimated ctDNA fraction of the liquid biopsy. Tumor fraction of tissue biopsy is listed on left. Table to the right lists short variants identified exclusively in tissue (orange), in both tissue and liquid (blue), or exclusively in liquid (green). Ratio of VAF/ctDNA fraction is listed in parentheses after each variant detected in liquid biopsy. *, VAF can exceed ctDNA fraction if mutation is an amplified copy of *AR*. **G,** Tissue–liquid pairs in which an *AR* amplification was detected in tissue. Correlation of copy number, ctDNA fraction, and detection in the matched liquid biopsy.

AR rearrangements that truncate the reading frame just after exon 3 yield a receptor with an intact DNA binding domain (DBD) and without a LBD to suppress its activity (51, 52). These rearrangements were detected in 160 patients (17% of AR-altered patients and 7% overall), more commonly than the 2.2% frequency detected among metastatic tissue samples (**Fig. 4E**; ref. 12). The number of intra-*AR* rearrangements was consistent with ctDNA from patients with mCRPC who have undergone ARSi therapy (52). There were 7 patients with truncating mutations in *AR* that disrupt the LBD and retain the DBD; these may yield active ARSi-resistant receptors according to similar principles (ref. 53; Supplementary Fig. S11A).

AR alterations were significantly more common among TRITON2 than TRITON3 screening samples (52% vs. 37%; $P = 3.0E\text{-}8$; Supplementary Table S4), consistent with progression on more lines of therapy and higher ctDNA fractions in the TRITON2 cohort. It is also possible that higher ctDNA fractions in the TRITON2 cohort allowed for more sensitive detection of certain variants, such as amplifications.

AR variants in liquid and tissue biopsies

Among patient-matched tissue/liquid sample pairs, liquid biopsy detected far more *AR* short variant mutations than tissue (18 shared, 10 tissue only, and 173 liquid only). To exclude pairs where tissue was archival and collected prior to exposure to ARSis, pairs collected within 30 days of each other were compared. Among these, 10 *AR* mutations were detected concordantly, three mutations exclusively in tissue, and 13 exclusively by liquid. In 7 of 17 patients, liquid biopsy provided the only evidence of *AR* mutations, and in 2 of 17 patient additional mutations were detected by liquid biopsy (**Fig. 4F**). This analysis highlights the ability of liquid biopsy to detect subclonal resistance variants that may not exist in every metastatic lesion, and thus, may not be detected in a tissue biopsy, but have relevance when choosing a course of treatment.

AR amplifications were detected in 72 of the tissue samples, with a median copy number of 20 (IQR, 13–35). Liquid biopsy detected 53% of these amplifications (38/72), and 91% of amplifications when ctDNA fraction was ≥20% (32/35). Amplifications with greater copy numbers could be detected at lower ctDNA fractions: liquid biopsy detected 87% of amplifications of copy number > 16 in samples with a ctDNA fraction as low as 5% (**Fig. 4G**). *AR* amplifications were detected exclusively in liquid biopsy in 96 samples. Among the 79 contemporaneously collected pairs where *AR* was profiled (**Table 1**), 20 amplifications were detected concordantly, 16 exclusively in tissue, and five exclusively in liquid. Lack of detection in liquid biopsy was largely attributable to ctDNA fractions below 20% (Supplementary Fig. S11B). In contemporaneous pairs, one *AR* rearrangement was detected concordantly and five exclusively in liquid (Supplementary Fig. S11C).

Discussion

In the largest study of mCRPC liquid biopsy samples conducted to date, CGP of liquid biopsies from 3,334 patients with advanced prostate cancer recapitulated the genomic landscape detected in tissue biopsies, with a high level of agreement in detection of *BRCA1/2* mutations. ctDNA also identified more acquired resistance alterations than tissue, including novel *AR*-activating alterations and subclonal *BRCA1/2* secondary mutations and reversions.

Analysis of cfDNA extracted from plasma was feasible in these cohorts, with 94% of patients having detectable ctDNA and with higher ctDNA fraction among patients with more advanced disease. The rich genomic signal within ctDNA, combined with its ease of use as compared with biopsy of a metastatic site, suggest that liquid biopsy could be a compelling option for identifying targetable GAs in patients with mCRPC.

A total of 94% of *BRCA1/2* mutations and 90% of all *BRCA1/2* variants detected by tissue CGP were detected in ctDNA, including all predicted germline variants. Liquid biopsy also demonstrated the ability to identify patients with somatic *BRCA2* mutations not detected in tissue, some with a high VAF, suggesting homologous recombination deficiency acquired later in tumor evolution. Given the high percentage of patients with detectable ctDNA and the agreement with tissue-defined genomic landscape of mCRPC observed in this study, CGP of a minimally invasive plasma biopsy is a viable option to detect *BRCA1/2* mutations. Of note, this analysis did not test for *BRCA1/2* homozygous deletion; this variant is more challenging to detect in ctDNA, but is measured on the latest version of the assay, which has recently been approved by the FDA (54). An estimated additional approximately 3% of patients with mCRPC might have been identified as having *BRCA1/2* mutations with a platform that reports deletions (12). These patients are worth identifying because they may receive particularly sustained benefit from PARPis, having a *BRCA* defect incapable of reversion (17, 55).

The most striking area of discordance between liquid and tissue variant detection was in the detection of a range of resistance mutations, in agreement with previous reports documenting the sensitivity of liquid biopsies in detecting *AR*-directed resistance mutations (27, 47, 48, 56–59). *AR*-activating alterations and subclonal somatic *BRCA1/2* secondary mutations and reversions were far more prevalent in liquid biopsies, likely due to a combination of (i) differences in the patient populations, because patients submitting a liquid biopsy likely were exposed to more lines of therapy (Supplementary Fig. S7A), (ii) the increased sensitivity of detection and lower reported VAFs in liquid biopsies over tissue testing, and (iii) the ability of liquid biopsy to integrate acquired resistance signals from multiple metastatic sites (**Fig. 4F**).

The sensitive detection of resistance mechanisms in liquid biopsies can potentially be used as a marker of therapy resistance and could provide additional ability to detect patients who might benefit from a non-ARSi drug. In this study, liquid biopsy outperformed tissue in detecting *AR* mutations that have relevance to clinical decisions about choices of ARSis, including W742L (bicalutamide resistance), H875Y and T878A (bicalutamide/enzalutamide/apalutamide resistance), and L702H (resistance to the AR proteolysis-targeting chimera ARV-110; refs. 45, 46). Liquid biopsy's sensitive detection of *BRCA1/2* reversions offers potential to be used for monitoring of emerging resistance.

One established limitation of liquid biopsy genotyping is the identification of mutations derived from white blood cells (e.g., clonal hematopoiesis; refs. 29, 31, 60), an age-related phenomenon which may be particularly relevant in patients with prostate cancer who tend to be older at metastatic diagnosis. Intuitively, alterations which confer a fitness advantage in hematopoietic progenitors (*JAK2* V617F and *IDH2* R140Q) are often suspected to originate from clonal hematopoiesis. Our study found an increased prevalence of mutations in *ATM* and *CHEK2* in ctDNA compared with tissue, two potentially targetable HRR genes that can be mutated in cancer cells, can harbor germline mutations, and have been described as recurrently mutated in clonal hematopoiesis (31, 61). Our study also identified enrichment for *NF1* and *TERT* promoter mutations in ctDNA. *NF1* inactivation has been detected in tumor-infiltrating lymphocytes and white blood cells in previous studies (31, 62). *TERT* promoter mutations have not been implicated as clonal hematopoiesis variants, but have been linked

to myeloid malignancies. These findings highlight that genomic discovery based on ctDNA genomics may benefit from paired-depth blood cell sequencing to clarify tumor-derived versus clonal hematopoiesis–derived signal. While such mutations are suspicious for clonal hematopoiesis, even classic clonal hematopoiesis genes may impact prostate cancer biology, with a recent study noting that *TET2* and *IDH1* are commonly altered in a novel subtype of prostate cancer (63). In clinical care, such paired-depth blood cell sequencing is not widely available, therefore, clinicians must understand, even when using FDA-approved assays, that clonal hematopoiesis mutations are common and mutations in *ATM* and *CHEK2* may not always be tumor derived.

The key limitation of ctDNA analysis is the variable shed of ctDNA into plasma. In this study, 60% of samples had a ctDNA fraction below 20%, which reduced the ability to detect amplifications. Both liquid biopsy platforms used in this study were not designed to detect deletions, leading to marked underdetection of PI3K signaling perturbation (*PTEN* homozygous deletions account for more than half of alterations in that gene, ∼30% to the 9% detected in this study). Other genes in the panel where deletions were likely missed were *RB1, BRCA1/2, APC*, and *TP53*. Deletions are captured with FMI's next-generation assay (54). Finally, the routine clinical CGP prostate cancer samples available for this study do not uniformly represent mCRPC, and there was limited information on treatments the patients received prior to specimen collection. Nevertheless, this dataset closely resembles the defined mCRPC TRITON2/3 cohorts and demonstrates the utility of liquid biopsy to identify patients who may benefit from targeted therapies.

This study highlights the ability of the liquid platform to detect targetable alterations in patients with mCRPC, including somatic mutations acquired during or after the transition to castration-resistant, metastatic disease. It also exposes some of the weaknesses of ctDNA analysis, such as reduced detection of copy-number changes in biopsies with low ctDNA. This reduced sensitivity with lower ctDNA content highlights that liquid biopsy cannot replace tissue CGP, but may complement it. If tissue profiling fails due to specimen inadequacy, the high ctDNA shed in prostate cancer means liquid biopsy could serve as a back-up. Alternatively, if tissue is unavailable for profiling, liquid biopsy could be used first with tissue CGP as a reflex option when ctDNA analysis is negative, indeed clinicians ordering a liquid biopsy might in parallel request archival tissue for CGP so this can be analyzed if ctDNA is uninformative. Together, these two diagnostic tools offer an opportunity to increase access to precision therapeutics in advanced prostate cancer.

Authors' Disclosures

H. Tukachinsky reported personal fees from Foundation Medicine and Roche during the conduct of the study. R.W. Madison reported personal fees from Foundation Medicine and other from Roche AG during the conduct of the study. J.H. Chung reported employment with Foundation Medicine. O.V. Gjoerup reported personal fees from Foundation Medicine and other from Roche during the conduct of the study and outside the submitted work. E.A. Severson reported personal fees from Foundation Medicine during the conduct of the study and outside the submitted work. L. Dennis reported other from Roche outside the submitted work. B.J. Fendler reported a patent for WO/2020/236941 pending. S. Morley reported personal fees from Foundation Medicine Inc. during the conduct of the study and outside the submitted work. L. Zhong reported personal fees from Foundation Medicine during the conduct of the study and outside the submitted work. R.P. Graf reported personal fees from Foundation Medicine during the conduct of the study. J.S. Ross reported personal fees from Foundation Medicine during the conduct of the study. B.M. Alexander reported personal fees from Foundation Medicine and Roche during the conduct of the study. W. Abida reported personal fees from Clovis Oncology during the conduct of the study. K. Fizazi reported nonfinancial support from Astellas, Bayer, Janssen, Sanofi, and MSD and personal fees from Clovis, CureVac, and Orion outside the submitted work. S.P. Watkins reported other from Clovis Oncology during the conduct of the study and outside the submitted work. A. Simmons reported other from Clovis Oncology during the conduct of the study. J.M. Venstrom reported other from Foundation Medicine during the conduct of the study, and other from Foundation Medicine and Roche outside the submitted work. G.R. Oxnard reported other from Foundation Medicine and Roche during the conduct of the study and personal fees from AstraZeneca, Takeda, Dropworks, Blueprint, Illumina, Inivata, Janssen, and AbbVie outside the submitted work. No disclosures were reported by the other authors.

Authors' Contributions

H. Tukachinsky: Conceptualization, data curation, formal analysis, investigation, visualization, writing–original draft, writing–review and editing. **R.W. Madison:** Conceptualization, data curation, formal analysis, investigation, visualization, writing–review and editing. **J.H. Chung:** Conceptualization, supervision, investigation, writing–review and editing. **O.V. Gjoerup:** Supervision, project administration, writing–review and editing. **E.A. Severson:** Resources, supervision, investigation, writing–review and editing. **L. Dennis:** Supervision, writing–review and editing. **B.J. Fendler:** Formal analysis, investigation, writing–review and editing. **S. Morley:** Resources, investigation, writing–review and editing. **L. Zhong:** Resources, investigation, writing–review and editing. **R.P. Graf:** Resources, investigation, writing–review and editing. **J.S. Ross:** Supervision, writing–review and editing. **B.M. Alexander:** Supervision, writing–review and editing. **W. Abida:** Resources, investigation, writing–review and editing. **S. Chowdhury:** Resources, Investigation, writing–review and editing. **C.J. Ryan:** Resources, investigation, writing–review and editing. **K. Fizazi:** Investigation, writing–review and editing. **T. Golsorkhi:** Investigation, writing–review and editing. **S.P. Watkins:** Resources, Investigation, writing–review and editing. **A. Simmons:** Resources, investigation, writing–review and editing. **A. Loehr:** Resources, investigation, writing–review and editing. **J.M. Venstrom:** Conceptualization, supervision, writing–review and editing. **G.R. Oxnard:** Conceptualization, supervision, writing–review and editing.

Acknowledgments

The TRITON2 and TRITON3 trials were funded by Clovis Oncology, Inc. We thank and acknowledge all patients and their families and caregivers who are participating in the trials, along with the investigators. We thank Brady Forcier and Jeff Lee for help with data analysis. We thank Neeru Bhardwaj for critical reading and helpful discussions of the article.

The costs of publication of this article were defrayed in part by the payment of page charges. This article must therefore be hereby marked *advertisement* in accordance with 18 U.S.C. Section 1734 solely to indicate this fact.

Received December 11, 2020; revised January 13, 2021; accepted February 3, 2021; published first February 8, 2021.

References

1. Bray F, Ferlay J, Soerjomataram I, Siegel RL, Torre LA, Jemal A. Global cancer statistics 2018: GLOBOCAN estimates of incidence and mortality worldwide for 36 cancers in 185 countries. CA Cancer J Clin 2018;68:394–424.
2. Kongseang C, Attawettayanon W, Kanchanawanichkul W, Pripatnanont C. Predictive factor of androgen deprivation therapy for patients with advanced stage prostate cancer. Prostate International 2017;5:35–8.
3. Nuhn P, de Bono JS, Fizazi K, Freedland SJ, Grilli M, Kantoff PW, et al. Update on systemic prostate cancer therapies: management of metastatic castration-resistant prostate cancer in the era of precision oncology. Eur Urol 2019;75:88–99.
4. de Wit R, de Bono J, Sternberg CN, Fizazi K, Tombal B, Wülfing C, et al. Cabazitaxel versus abiraterone or enzalutamide in metastatic prostate cancer. N Engl J Med 2019;381:2506–18.

5. Oh WK, Cheng WY, Miao R, Vekeman F, Gauthier-Loiselle M, Duh MS, et al. Real-world outcomes in patients with metastatic castration-resistant prostate cancer receiving second-line chemotherapy versus an alternative androgen receptor-targeted agent (ARTA) following early progression on a first-line ARTA in a US community oncology setting. Urol Oncol 2018;36:500.e1–9.
6. Francini E, Gray KP, Shaw GK, Evan CP, Hamid AA, Perry CE, et al. Impact of new systemic therapies on overall survival of patients with metastatic castration-resistant prostate cancer in a hospital-based registry. Prostate Cancer Prostatic Dis 2019;22:420–7.
7. Abeshouse A, Ahn J, Akbani R, Ally A, Amin S, Andry CD, et al. The molecular taxonomy of primary prostate cancer. Cell 2015;163:1011–25.
8. Beltran H, Yelensky R, Frampton GM, Park K, Downing SR, MacDonald TY, et al. Targeted next-generation sequencing of advanced prostate cancer identifies potential therapeutic targets and disease heterogeneity. Eur Urol 2013;63:920–6.
9. Robinson D, van Allen EM, Wu YM, Schultz N, Lonigro RJ, Mosquera JM, et al. Integrative clinical genomics of advanced prostate cancer. Cell 2015; 161:1215–28.
10. Abida W, Armenia J, Gopalan A, Brennan R, Walsh M, Barron D, et al. Prospective genomic profiling of prostate cancer across disease states reveals germline and somatic alterations that may affect clinical decision making. JCO Precis Oncol 2017;2017:PO.17.00029.
11. Armenia J, Wankowicz SAM, Liu D, Gao J, Kundra R, Reznik E, et al. The long tail of oncogenic drivers in prostate cancer. Nat Genet 2018;50:645–51.
12. Chung JH, Dewal N, Sokol E, Mathew P, Whitehead R, Millis SZ, et al. Prospective comprehensive genomic profiling of primary and metastatic prostate tumors. JCO Precis Oncol 2019;3:PO.18.00283.
13. Mateo J, Seed G, Bertan C, Rescigno P, Dolling D, Figueiredo I, et al. Genomics of lethal prostate cancer at diagnosis and castration resistance. J Clin Invest 2020; 130:1743–51.
14. Mateo J, Carreira S, Sandhu S, Miranda S, Mossop H, Perez-Lopez R, et al. DNA-repair defects and olaparib in metastatic prostate cancer. N Engl J Med 2015;373: 1697–708.
15. Mateo J, Porta N, Bianchini D, McGovern U, Elliott T, Jones R, et al. Olaparib in patients with metastatic castration-resistant prostate cancer with DNA repair gene aberrations (TOPARP-B): a multicentre, open-label, randomised, phase 2 trial. Lancet Oncol 2020;21:162–74.
16. Abida W, Campbell D, Patnaik A, Shapiro JD, Sautois B, Vogelzang NJ, et al. Non-BRCA DNA damage repair gene alterations and response to the PARP inhibitor rucaparib in metastatic castration-resistant prostate cancer: analysis from the phase 2 TRITON2 study. Clin Cancer Res 2020;26:2487–96.
17. Abida W, Campbell D, Patnaik A, Sautois B, Shapiro JD, Vogelzang NJ, et al. Genomic characteristics associated with clinical activity of rucaparib in patients (pts) with BRCA1 or BRCA2 (BRCA) - mutated metastatic castration-resistant prostate cancer (mCRPC). J Clin Oncol 2020;38:178.
18. Pilarski R. The role of BRCA testing in hereditary pancreatic and prostate cancer families. Am Soc Clin Oncol Educ Book 2019;39:79–86.
19. Pritchard CC, Mateo J, Walsh MF, de Sarkar N, Abida W, Beltran H, et al. Inherited DNA-repair gene mutations in men with metastatic prostate cancer. N Engl J Med 2016;375:443–53.
20. de Bono JS, de Giorgi U, Rodrigues DN, Massard C, Bracarda S, Font A, et al. Randomized phase II study evaluating AKT blockade with ipatasertib, in combination with abiraterone, in patients with metastatic prostate cancer with and without PTEN loss. Clin Cancer Res 2019;25:928–36.
21. Abida W, Cheng ML, Armenia J, Middha S, Autio KA, Vargas HA, et al. Analysis of the prevalence of microsatellite instability in prostate cancer and response to immune checkpoint blockade. JAMA Oncol 2019;5:471–8.
22. Wu YM, Cies´lik M, Lonigro RJ, Vats P, Reimers MA, Cao X, et al. Inactivation of CDK12 delineates a distinct immunogenic class of advanced prostate cancer. Cell. 2018;173:1770–82.
23. Wong SK, Mohamad NV, Giaze TR, Chin KY, Mohamed N, Ima-Nirwana S. Prostate cancer and bone metastases: the underlying mechanisms. Int J Mol Sci 2019;20:2587.
24. Gandaglia G, Abdollah F, Schiffmann J, Trudeau V, Shariat SF, Kim SP, et al. Distribution of metastatic sites in patients with prostate cancer: a population-based analysis. Prostate 2014;74:210–6.
25. Sailer V, Schiffman MH, Kossai M, Cyrta J, Beg S, Sullivan B, et al. Bone biopsy protocol for advanced prostate cancer in the era of precision medicine. Cancer 2018;124:1008–15.
26. Lorente D, Omlin A, Zafeiriou Z, Nava-Rodrigues D, Pérez-López R, Pezaro C, et al. Castration-resistant prostate cancer tissue acquisition from bone metastases for molecular analyses. Clin Genitourin Cancer 2016;14:485–93.
27. Wyatt AW, Azad AA, Volik SV, Annala M, Beja K, McConeghy B, et al. Genomic alterations in cell-free DNA and enzalutamide resistance in castration-resistant prostate cancer. JAMA Oncol 2016;2:1598–606.
28. Wyatt AW, Annala M, Aggarwal R, Beja K, Feng F, Youngren J, et al. Concordance of circulating tumor DNA and matched metastatic tissue biopsy in prostate cancer. J Natl Cancer Inst 2017;109:djx118.
29. Mayrhofer M, de Laere B, Whitington T, van Oyen P, Ghysel C, Ampe J, et al. Cell-free DNA profiling of metastatic prostate cancer reveals microsatellite instability, structural rearrangements and clonal hematopoiesis. Genome Med 2018;10:85.
30. Sonpavde G, Agarwal N, Pond GR, Nagy RJ, Nussenzveig RH, Hahn AW, et al. Circulating tumor DNA alterations in patients with metastatic castration-resistant prostate cancer. Cancer 2019;125:1459–69.
31. Razavi P, Li BT, Brown DN, Jung B, Hubbell E, Shen R, et al. High-intensity sequencing reveals the sources of plasma circulating cell-free DNA variants. Nat Med 2019;25:1928–37.
32. Clark TA, Chung JH, Kennedy M, Hughes JD, Chennagiri N, Lieber DS, et al. Analytical validation of a hybrid capture–based next-generation sequencing clinical assay for genomic profiling of cell-free circulating tumor DNA. J Mol Diagn 2018;20:686–702.
33. Gowen K, Clark TA, Gregg JP, Greene MZ, Murphy A, White J, et al. MSI-H testing via hybrid capture based NGS sequencing of liquid biopsy samples. J Clin Oncol 2019;37:504.
34. Sun JX, He Y, Sanford E, Montesion M, Frampton GM, Vignot S, et al. A computational approach to distinguish somatic vs. germline origin of genomic alterations from deep sequencing of cancer specimens without a matched normal. PLoS Comput Biol 2018;14:e1005965.
35. Sokol ES, Pavlick D, Khiabanian H, Frampton GM, Ross JS, Gregg JP, et al. Pan-cancer analysis of BRCA1 and BRCA2 genomic alterations and their association with genomic instability as measured by genome-wide loss of heterozygosity. JCO Precis Oncol 2020;4:442–65.
36. Annala M, Vandekerkhove G, Khalaf D, Taavitsainen S, Beja K, Warner EW, et al. Circulating tumor DNA genomics correlate with resistance to abiraterone and enzalutamide in prostate cancer. Cancer Discov 2018;8: 444–57.
37. Abida W, Cyrta J, Heller G, Prandi D, Armenia J, Coleman I, et al. Genomic correlates of clinical outcome in advanced prostate cancer. Proc Natl Acad Sci U S A 2019;166:11428–36.
38. Gallo LH, Nelson KN, Meyer AN, Donoghue DJ. Functions of fibroblast growth factor receptors in cancer defined by novel translocations and mutations. Cytokine Growth Factor Rev 2015;26:425–49.
39. Xie M, Lu C, Wang J, McLellan MD, Johnson KJ, Wendl MC, et al. Age-related mutations associated with clonal hematopoietic expansion and malignancies. Nat Med 2014;20:1472–8.
40. Nientiedt C, Heller M, Endris V, Volckmar AL, Zschäbitz S, Tapia-Laliena MA, et al. Mutations in BRCA2 and taxane resistance in prostate cancer. Sci Rep 2017; 7:1–10.
41. Castro E, Romero-Laorden N, del Pozo A, Lozano R, Medina A, Puente J, et al. PROREPAIR-B: a prospective cohort study of the impact of germline DNA repair mutations on the outcomes of patients with metastatic castration-resistant prostate cancer. J Clin Oncol 2019;37:490–503.
42. Quigley D, Alumkal JJ, Wyatt AW, Kothari V, Foye A, Lloyd P, et al. Analysis of circulating cell-free DNA identifies multiclonal heterogeneity of BRCA2 reversion mutations associated with resistance to PARP inhibitors. Cancer Discov 2017;7:999–1005.
43. Cheng HH, Salipante SJ, Nelson PS, Montgomery B, Pritchard CC. Polyclonal BRCA2 reversion mutations detected in circulating tumor DNA after platinum chemotherapy in a patient with metastatic prostate cancer. JCO Precis Oncol 2018;2:PO.17.00169.
44. Simmons AD, Nguyen M, Pintus E. Polyclonal BRCA2 mutations following carboplatin treatment confer resistance to the PARP inhibitor rucaparib in a patient with mCRPC: a case report. BMC Cancer 2020;20:215.
45. Lallous N, Volik SV, Awrey S, Leblanc E, Tse R, Murillo J, et al. Functional analysis of androgen receptor mutations that confer anti-androgen resistance identified in circulating cell-free DNA from prostate cancer patients. Genome Biol 2016;17:10.
46. Proof-of-concept with PROTACs in prostate cancer. Cancer Discov 2020;10: 1084. DOI: 10.1158/2159-8290.CD-NB2020-054. Available from: https://pubmed.ncbi.nlm.nih.gov/32503798.
47. Sumiyoshi T, Mizuno K, Yamasaki T, Miyazaki Y, Makino Y, Okasho K, et al. Clinical utility of androgen receptor gene aberrations in circulating cell-free

DNA as a biomarker for treatment of castration-resistant prostate cancer. Sci Rep 2019;9:4030.
48. Azad AA, Volik SV, Wyatt AW, Haegert A, le Bihan S, Bell RH, et al. Androgen receptor gene aberrations in circulating cell-free DNA: biomarkers of therapeutic resistance in castration-resistant prostate cancer. Clin Cancer Res 2015;21:2315–24.
49. Prekovic S, van Royen ME, Voet ARD, Geverts B, Houtman R, Melchers D, et al. The effect of F877L and T878A mutations on androgen receptor response to enzalutamide. Mol Cancer Ther 2016;15:1702–12.
50. An J, Wang C, Deng Y, Yu L, Huang H. Destruction of full-length androgen receptor by wild-type SPOP, but not prostate-cancer-associated mutants. Cell Rep 2014;6:657–69.
51. Nyquist MD, Li Y, Hwang TH, Manlove LS, Vessella RL, Silverstein KAT, et al. TALEN-engineered AR gene rearrangements reveal endocrine uncoupling of androgen receptor in prostate cancer. Proc Natl Acad Sci U S A 2013; 110:17492–7.
52. Henzler C, Li Y, Yang R, McBride T, Ho Y, Sprenger C, et al. Truncation and constitutive activation of the androgen receptor by diverse genomic rearrangements in prostate cancer. Nat Commun 2016;7:1–12.
53. Han D, Gao S, Valencia K, Owiredu J, Han W, de Waal E, et al. A novel nonsense mutation in androgen receptor confers resistance to CYP17 inhibitor treatment in prostate cancer. Oncotarget 2017;8:6796–808.
54. Woodhouse R, Dennis L, Li M, Burns C, Ma P, Meng W, et al. Clinical and analytical validation of FoundationOne Liquid CDx, a novel 324-gene blood-based comprehensive genomic profiling assay. J Clin Oncol 2020;38:e13685.
55. Antonarakis ES, Madison R, Snider J, Snow T, Sokol E, Chung J, et al. Association of BRCA alteration (alt) type with real-world (RW) outcomes to PARP inhibitors (PARPi) in patients (pts) with metastatic castrate-resistant prostate cancer (mCRPC). J Clin Oncol 2020;38:5527.
56. Conteduca V, Wetterskog D, Sharabiani MTA, Grande E, Fernandez-Perez MP, Jayaram A, et al. Androgen receptor gene status in plasma DNA associates with worse outcome on enzalutamide or abiraterone for castration-resistant prostate cancer: a multi-institution correlative biomarker study. Ann Oncol 2017;28:1–9.
57. Conteduca V, Jayaram A, Romero-Laorden N, Wetterskog D, Salvi S, Gurioli G, et al. Plasma androgen receptor and docetaxel for metastatic castration-resistant prostate cancer. Eur Urol 2019;75:368–73.
58. Torquato S, Pallavajjala A, Goldstein A, Valda Toro P, Silberstein JL, Lee J, et al. Genetic alterations detected in cell-free DNA are associated with enzalutamide and abiraterone resistance in castration-resistant prostate cancer. JCO Precis Oncol 2019;3:1–14.
59. Kohli M, Tan W, Zheng T, Wang A, Montesinos C, Wong C, et al. Clinical and genomic insights into circulating tumor DNA-based alterations across the spectrum of metastatic hormone-sensitive and castrate-resistant prostate cancer. EBioMedicine 2020;54:102728.
60. Hu Y, Ulrich BC, Supplee J, Kuang Y, Lizotte PH, Feeney NB, et al. False-positive plasma genotyping due to clonal hematopoiesis. Clin Cancer Res 2018;24:4437–43.
61. Jensen K, Konnick EQ, Schweizer MT, Sokolova AO, Grivas P, Cheng HH, et al. Association of clonal hematopoiesis in DNA repair genes with prostate cancer plasma cell-free DNA testing interference. JAMA Oncol 2021;7:107–10.
62. Ptashkin RN, Mandelker DL, Coombs CC, Bolton K, Yelskaya Z, Hyman DM, et al. Prevalence of clonal hematopoiesis mutations in tumor-only clinical genomic profiling of solid tumors. JAMA Oncol 2018;4:1589–93.
63. Zhao SG, Chen WS, Li H, Foye A, Zhang M, Sjamp M, et al. The DNA methylation landscape of advanced prostate cancer. Nat Genet 2020;52: 778–89.